fact, the observed strong variation of the electronic interaction between molecule and substrate may be interpreted as repeated bond formation and breaking. If we analyse a particular scan line (compare top and bottom parts of Fig. 3a), we find that a given local density of states (that is, brightness) is without exception associated with (nearly) equivalent lattice positions on the underlying substrate. Thus, the molecule 'jumps' from adsorption site to adsorption site, always in the direction defined by the motion of the tip, while the range of the jump is determined by the relative orientation of the scanning direction and the crystallographic axes. The tip never loses control over the molecule, but the latter transiently binds to the substrate before being moved on. The fact that in this way the underlying lattice of silver is imaged unambiguously signals recognition of a specific site by perylene on Ag(111) and is thus equivalent to commensurability in condensed layers. We have therefore found conditions under which the weak reaction centre of perylene allows site recognition. The spectroscopic data indicating a weak bond between Ag(111) and perylene are thus fully confirmed by an independent technique[29] which is able to probe site recognition reactions even in cases where these are in strong competition with other influences, for example, intermolecular interactions. In fact, the tip suppresses the latter by forcing the apex molecule to sample the surface potential systematically.

The comparison of PTCDA with perylene proves the feasibility of effective control over epitaxial site recognition. In both molecules, the perylene backbone merely supplies potential for an efficient recognition centre. This potential is fully developed only if electronegative side groups, which increase the activity of the centre, are attached to the backbone. Side-group substitution is thus an important strategy for establishing control over organic epitaxy. In the present case, in going from perylene to PTCDA, the activity is enhanced by a factor of 300 if measured in terms of relative spectroscopic activities. We anticipate that this demonstrated insight into and control of site recognition sensitivities could be used not only in the context of organic epitaxy, but also whenever molecule–substrate interactions are intended as driving forces for structuring assemblies of large π-conjugated molecules at the nanoscale. □

Received 20 January; accepted 10 July 2003; doi:10.1038/nature01901.

1. Dodabalapur, A. Organic light emitting diodes. *Solid State Commun.* **102,** 259–267 (1997).
2. Horowitz, G. Organic field-effect transistors. *Adv. Mater.* **10,** 365–377 (1998).
3. Dimitrakopoulos, C. D. & Malenfant, P. R. L. Organic thin film transistors for large area electronics. *Adv. Mater.* **14,** 99–117 (2002).
4. Katz, H. E. *et al.* A soluble and air-stable organic semiconductor with high electron mobility. *Nature* **404,** 478–481 (2000).
5. Schoonfeld, W. A. *et al.* Coloumb-blockade transport in single-crystal organic thin-film transistors. *Nature* **404,** 977–980 (2000).
6. Crone, B. *et al.* Large-scale complementary integrated circuits based on organic transistors. *Nature* **403,** 521–523 (2000).
7. Dimitrakopoulos, C. D. *et al.* Low voltage organic transistors on plastic comprising high-dielectric constant gate insulators. *Science* **283,** 822–824 (1999).
8. Horowitz, G. *et al.* Role of semiconductor/insulator interface in the characteristics of π-conjugated-oligomer-based thin film transistors. *Synth. Metals* **51,** 419–424 (1992).
9. Hill, I. G. *et al.* Organic semiconductor interfaces: electronic structure and transport properties. *Appl. Surf. Sci.* **166,** 354–362 (2000).
10. Meyer zu Heringdorf, F. J. *et al.* Growth dynamics of pentacene films. *Nature* **412** (2001), 517–520.
11. Forrest, S. R. Ultrathin organic films grown by molecular beam deposition and related techniques. *Chem. Rev.* **97,** 1793–1896 (1997).
12. Hillier, A. C. & Ward, M. D. Epitaxial interactions between molecular overlayers and ordered substrates. *Phys. Rev. B* **54,** 14037–14051 (1996).
13. Umbach, E. *et al.* Surface architecture with large organic molecules: Interface order and epitaxy. *Surf. Sci.* **402–404,** 20–31 (1998).
14. Chen, Q. *et al.* Epitaxy of a crystalline organic semiconductor: Perylene/Cu(110). *Chem. Mater.* **14,** 743–749 (2002).
15. Fink, R. *et al.* Substrate-dependent lateral order in naphthalene-tetracarboxylic-dianhydride monolayers. *Phys. Rev. B* **60,** 2818–2826 (1999).
16. Soukopp, A. *et al.* Superstructure formation of large organic adsorbates on a metal surface: A systematic approach using oligothiophenes on Ag(111). *Phys. Rev. B* **58,** 13882–13894 (1998).
17. Tada, H. *et al.* Structural analysis of lead phthalocyanine ultrathin films grown on cleaved faces of alkali halides by reflection high energy electron diffraction. *Surf. Sci.* **268,** 387–396 (1992).
18. Zhang, Y. & Forrest, S. R. Mechanisms of quasiepitaxial ordering at organic molecular thin film interfaces. *Phys. Rev. Lett.* **71,** 2765–2768 (1993).
19. Forrest, S. R. *et al.* Ultrahigh-vacuum quasiepitaxial growth of model van der Waals thin films II. Experiment. *Phys. Rev. B* **49,** 11309–11321 (1994).
20. Hirose, Y. *et al.* Ordered, quasi-epitaxial growth of organic thin film on Se-passivated GaAs(100). *Appl. Phys. Lett.* **66,** 944–946 (1995).
21. Schmitz-Huebsch, T. *et al.* Epitaxial growth of 3,4,9,10-perylenetetracarboxylic dianhydride on Au(111): A STM and RHEED study. *Phys. Rev. B* **55,** 7972–7976 (1997).
22. Hirose, Y. *et al.* Quasiepitaxial growth of the organic molecular semiconductor 3,4,9,10-perylenetetracarboxylic dianhydride. *Phys. Rev. B* **52,** 14040–14047 (1995).
23. Forrest, S. R. *et al.* Organic-on-organic semiconductor contact barrier diodes. II. Dependence on organic film and metal contact properties. *J. Appl. Phys.* **56** 543–551 (1984),.
24. Möbus, M. *et al.* Structure of perylene-tetracarboxylic-dianhydride thin films on alkali halide crystal substrates. *J. Cryst. Growth* **116,** 495–504 (1992).
25. Taborski, J. *et al.* NEXAFS investigations on ordered adsorbate layers of large aromatic molecules. *J. Electr. Spec. Rel. Phenom.* **75,** 129–147 (1995).
26. Tautz, F. S. *et al.* Strong electron-phonon-coupling at a metal/organic interface: PTCDA/Ag(111). *Phys. Rev. B* **65,** 125405 (2002).
27. Tautz, F. S. *et al.* A comparison of the chemisorption behaviour of PTCDA on different Ag surfaces. *Surf. Sci.* **502–503,** 176–184 (2002).
28. Frisch, M. *et al. Gaussian 98, Rev. A6*, (1998) (Gaussian, Inc., Pittsburgh).
29. Böhringer, M. *et al.* Scanning tunneling microscope-induced molecular motion and its effect on the image formation. *Surf. Sci.* **408,** 72–85 (1998).
30. Wagner, V. Raman analysis of ordered organic monolayers on metal surfaces. *Phys. Status Solidi A* **188,** 1297–1305 (2001).

Acknowledgements We thank V. Shklover and E. Umbach of the University of Würzburg for making output data of the quantum chemical calculations available to us, and for discussions. The work was financially supported by the Deutsche Forschungsgemeinschaft.

Competing interests statement The authors declare that they have no competing financial interests.

Correspondence and requests for materials should be addressed to F.S.T. (s.tautz@iu-bremen.de).

Growth of early continental crust by partial melting of eclogite

Robert P. Rapp[1]*, Nobumichi Shimizu[2] & Marc D. Norman[3]

[1]*Mineral Physics Institute and Department of Geosciences, State University of New York at Stony Brook, Stony Brook, New York 11794-2100, USA*
[2]*Department of Geology and Geophysics, Woods Hole Oceanographic Institution, Woods Hole, Massachusetts 02543, USA*
[3]*Research School of Earth Sciences, Australian National University, Canberra, ACT 0200, Australia*

* Present address: Geodynamics Research Center, Ehime University, 2-5 Bunkyo-cho, Matsuyama 790-8577 Japan

The tectonic setting in which the first continental crust formed, and the extent to which modern processes of arc magmatism at convergent plate margins were operative on the early Earth, are matters of debate[1,2]. Geochemical studies have shown that felsic rocks in both Archaean high-grade metamorphic ('grey gneiss') and low-grade granite-greenstone terranes are comprised dominantly of sodium-rich granitoids of the tonalite-trondhjemite-granodiorite (TTG) suite of rocks[3–7]. Here we present direct experimental evidence showing that partial melting of hydrous basalt in the eclogite facies produces granitoid liquids with major- and trace-element compositions equivalent to Archaean TTG, including the low Nb/Ta and high Zr/Sm ratios of 'average' Archaean TTG[8], but from a source with initially subchondritic Nb/Ta. In modern environments, basalts with low Nb/Ta form by partial melting of subduction-modified depleted mantle[9,10], notably in intraoceanic arc settings in the forearc[11,12] and back-arc[13,14] regimes. These observations suggest that TTG magmatism may have taken place beneath granite-greenstone complexes developing along Archaean intraoceanic island arcs by imbricate thrust-stacking[15] and tectonic accretion[16] of a diversity of

subduction-related terranes. Partial melting accompanying dehydration of these generally basaltic source materials at the base of thickened, 'arc-like' crust would produce compositionally appropriate TTG granitoids in equilibrium with eclogite residues.

The trace-element characteristics of Archaean granitoids are almost universally used to draw inferences on the origins of Earth's earliest continental crust[1–7]. It is well established from melting/phase equilibria experiments on natural and synthetic basalts that liquids compositionally similar to TTG in terms of major-element oxide components form by low–moderate degree melting of mafic crust (basalt) in the amphibolite, garnet-amphibolite, or eclogite facies[17–20]. These experiments have provided data on the identity and proportions of coexisting residual (crystalline) phases, allowing for trace-element modelling of TTG petrogenesis when combined with available experimentally determined mineral-melt partition coefficients (*D* values) for amphibole, clinopyroxene and garnet.

Recently, a number of experimental studies have reported mineral-melt *D* values specific to TTG petrogenesis, that is, for tonalitic liquids in equilibrium with amphibolitic or eclogitic phase assemblages[21–23], measured in synthetic or natural systems but generally at trace-element concentrations well above natural abundance levels, to facilitate analysis by a variety of microbeam analytical techniques. In particular, partitioning data for the elements Nb, Ta, Zr and Sm have been used to develop a model for the origin of Earth's earliest continental crust, in which it is argued that only low-degree (~1–15%) melting of recycled (that is, subducted) oceanic crust in the form of amphibolite, a relatively low-pressure equivalent of hydrous basalt, can account for the high Zr/Sm and low Nb/Ta ratios that are assumed to be representative of 'average' Archaean TTG[8]. These conclusions are predicated on the presumption of an 'average' basaltic source material for Archaean TTG with a chondritic Nb/Ta ratio, discounting alternative scenarios for the petrogenesis of TTG in which melting accompanying the progressive dehydration of overthickened and/or subducted mafic crust would peak at somewhat greater depths, where crystalline residues would be comprised of eclogite.

Here we report combined ion-microprobe and laser-ablation data from inductively coupled plasma mass spectrometry (ICP-MS) for a number of key trace elements (including Nb, Ta, Zr and Sm), measured at natural abundance levels, for TTG liquids formed by partial melting of natural metabasalt at 2–4 GPa, and coexisting with eclogitic residues (see Methods section). We argue that TTG melts in equilibrium with eclogite residues, while satisfying 'first-order' trace-element constraints, are better able to account for the major-element compositional features of TTG than are amphibolitic residues. Furthermore, if one allows for compositional variability in the putative basaltic source for TTG, as observed for basalts from a diversity of subduction-related environments, then TTG melts in equilibrium with eclogitic residues also pass the 'critical test'[8], possessing appropriately low (yet variable) Nb/Ta ratios.

First-order geochemical characteristics of Archaean TTG include strong fractionation of light rare-earth elements (such as La) from heavy rare-earth elements (such as Yb), and Sr from Y, coupled to relative depletions in Yb and Y, resulting in high La/Yb and Sr/Y ratios[1–7,17]. These are features shared by the experimental TTG melts in equilibrium with eclogite, as well as their mantle-hybridized counterparts (Fig. 1), and are explicable in terms of the *D* values for these elements between eclogitic phases and TTG melts. For example, Sr and La are highly incompatible in both garnet and clinopyroxene (that is, mineral-melt *D* values $\ll 1.0$), whereas the heavy rare-earth elements (for example, Dy, Er and Yb) and Y are strongly compatible in garnet (*D* values $\gg 1.0$). As a consequence, TTG granitoids in equilibrium with eclogite possess characteristically high La/Yb and Sr/Y ratios[1,3–7,17]. By contrast, the *D* values for La and Sr betweem amphibole and TTG melt are an order of magnitude higher than those between garnet and TTG melt, and the *D* values for Y and Yb are an order of magnitude lower than those between garnet and TTG melt. Thus an amphibole-dominated residue will be less capable of imparting the high Sr/Y and La/Yb ratios and strong depletions in Yb and Y that are characteristic of Archaean TTG[1,5–7]. Our experimental liquids fall well within the field defined by early–late Archaean TTG for other trace elements as well, for example, Th and U (Fig. 2).

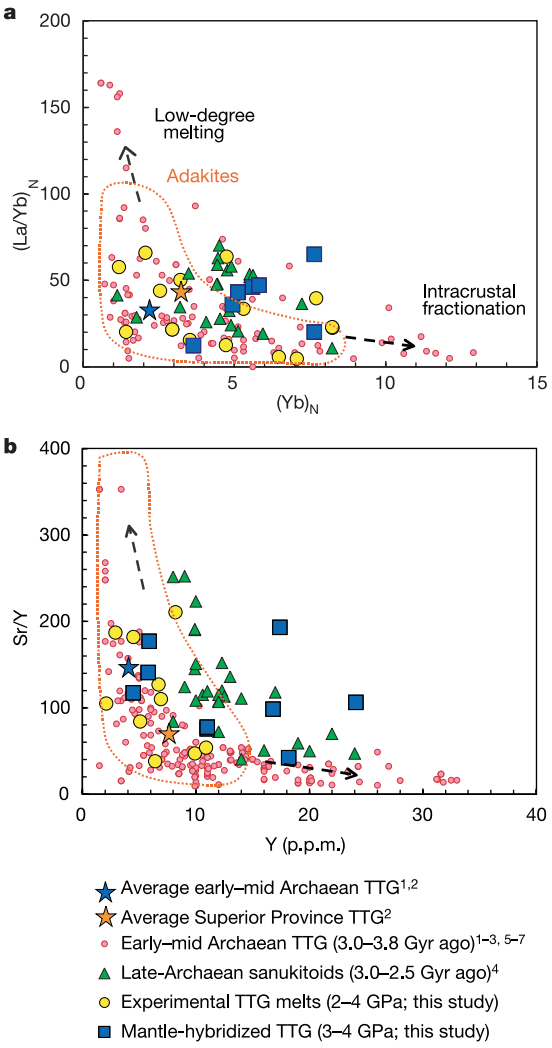

Figure 1 Selected trace-element ratios in early–mid-Archaean TTG and late Archaean sanukitoids[1–7] match those of experimental liquids in equilibrium with eclogite. Data for 'pristine' TTG melts in equilibrium with eclogite (Mg-number ≈ 0.30–0.50) at 2–4 GPa (refs 18, 20), and 'mantle-hybridized' TTG (Mg-number ≈ 50–70) in equilibrium with garnet websterite mineral assemblages at 3.5–4.0 GPa from ref. 19 and R.P.R. and N.S., unpublished data. Also shown is the field for adakite lavas (orange dotted line) in modern subduction zones[1], and the predicted effects of intracrustal differentiation by fractionation of amphibole and plagioclase at low pressure (black arrows)[1,5,6]. All experimental data for 'mantle-hybridized' from ref. 19 and R.P.R. and N.S., unpublished data; and for TTG liquids at 1.2–3.2 GPa from ref. 18, and unpublished data for additional peridotite assimilation experiments at 3–4 GPa. **a**, Plot of $(La/Yb)_N$ versus $(Yb)_N$, normalized to chondritic values. Extreme values of $(La/Yb)_N$ result from very low-degree melting of metabasaltic sources, and low $(La/Yb)_N$ ratios coupled with low Yb abundances from intracrustal fractionation of plagioclase and amphibole[1]. **b**, Plot of Sr/Y versus Y for the same data sets. Bulk distribution coefficients for TTG melts in equilibrium with eclogite residues account for the highly incompatible behaviour of both La and Sr, and the highly compatible behaviour of Y and Yb, which are strongly partitioned into garnet[8,21–23].

The major-element compositions of the great majority of Archaean TTG are characterized by SiO_2 contents of 65–73 wt% and Mg-numbers of 0.30–0.50 (where Mg-number = molar Mg/(Mg + Fe*)), and alumina saturation indexes (ASI, or A/CNK) of approximately 1.0 ± 0.05 (where A/CNK = molar $Al_2O_3/(CaO + Na_2O + K_2O)$[1–7]. These features (in particular, A/CNK ratios of ~1.0) require relatively high degrees of melting (>10–15%) of a garnet-bearing basaltic protolith, at pressure–temperature (*P*–*T*) conditions close to or beyond the 'amphibole-out' phase boundary[20], where amphibole will either be entirely absent from the eclogite residue, or a minor phase. By contrast, amphibole-dominated residues of hydrous basalt melting possess Mg-numbers generally below 0.30, and A/CNK ratios >1.1 (refs 17, 18, 20).

The argument for an origin for TTG by partial melting of an amphibolite source hinges largely on the ability of amphibole to fractionate Nb from Ta[8], and thereby to explain the low (subchondritic) Nb/Ta ratio of 'average' Archaean TTG, by assuming a source with initially chondritic Nb/Ta. In fact, as argued below, Archaean TTG, as well as their potential basaltic source materials, show a very wide range in Nb/Ta ratios.

A trend to lower Nb/Ta ratios has been documented for near-axis seamounts in the eastern Pacific[9], for oceanic crust formed in back-arc basins[13,14], for some boninites formed in the fore-arc region[11,12], and for "boninite-like" basalts in Archaean greenstone belts[24,31], including 3.7–3.8 Gyr old mafic volcanics from the Isua greenstone belt in West Greenland (ref. 31 and A. Polat, personal communication, 2002). In the Eastern Pacific seamounts, this trend is attributed to contamination of the upper mantle source region for these basalts by material that had been "processed" through a subduction zone[9], and for back-arc basin basalts, boninites and boninite-like rocks in Archaean greenstone belts, to enrichment of their mantle sources by slab-derived fluids possessing low Nb/Ta (refs 9–12). We consider our starting basalt AB-1 (see Table 1 and ref. 19) to be compositionally representative of basalts formed in marginal (back-arc) basins, generally subduction-enriched oceanic crust, boninitic lavas from fore-arc environments, and some greenstone belt metavolcanics that resemble these rocks compositionally

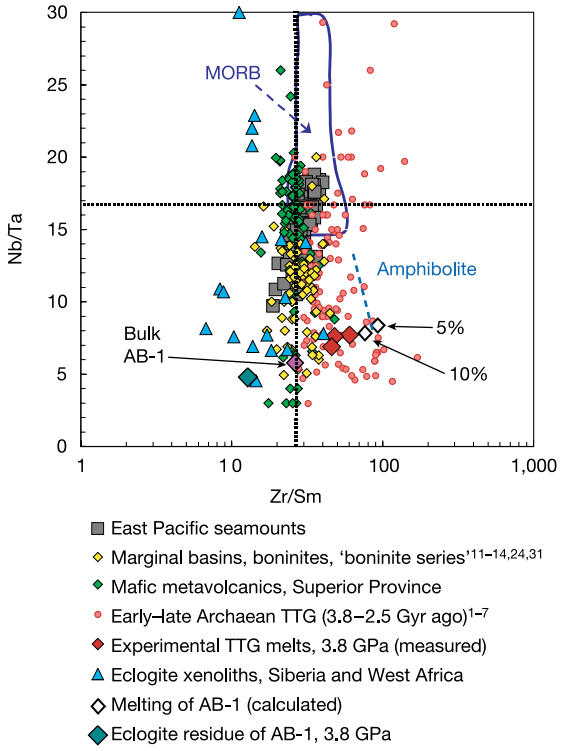

Figure 3 Niobium/tantalum versus zirconium/samarium ratios suggest a compositionally variable oceanic basaltic source for early–late-Archaean TTG magmas. Archaean TTGs include data from West Greenland (3.8 Gyr ago), the Kaapvaal (3.5–3.6 Gyr ago) and Zimbabwean (3.4 Gyr ago) cratons, the West African Craton (~3.5 Gyr ago), the Pilbara Craton (~3.5 Gyr ago), and the late-Archaean (~2.5–3.0 Gyr ago) Slave and Superior provinces of Canada[1–7]. These data are shown relative to possible basaltic source materials in Archaean greenstone belts, and their modern analogues, including seamounts from the eastern Pacific[9], intraoceanic basalts, including marginal basin basalts from the western Pacific[13,14], Phanerozoic boninites[11,12] and Archaean boninite-like or boninite series rocks[24,31]. Experimental data are shown for experimental TTG liquid formed by 30% melting of AB-1 and mantle-hybridized equivalents of the TTG-liquid at 30% melting, formed by assimilation of peridotite[19] (measured by laser ablation ICP-MS; see Table 1), as well as for 10% and 5% melting of AB-1 (calculated). Range of ratios from partitioning calculations of ref. 8 for 1–15% partial melting of amphibolite at 0.8 GPa are shown as light-blue bars. Initial variations in the Nb/Ta ratio of parental TTG magmas would reflect primarily the (variable) Nb/Ta ratio of their basaltic source(s). For TTG derived by eclogite melting of basaltic sources with bulk Nb/Ta ratios higher than AB-1 (~7–17), post-emplacement fractionation of amphibole would be able to reduce the Nb/Ta ratio of derivative magmas somewhat. Alternatively, small amounts of residual amphibole in the source (that is, melting of garnet amphibolite) would produce TTG liquids with Nb/Ta ratios slightly lower than the initial Nb/Ta ratio of the source. Eclogites interpreted as residues of TTG magmatism[26,27] show a range of Nb/Ta ratios consistent with our model, in which the basaltic source protolith possesses a range of initial Nb/Ta ratios. This protolith could be mafic arc crust formed in intraoceanic subduction zones, or oceanic crust whose source itself contains components of crust that had been recycled, perhaps repeatedly, through a more primitive subduction regime in the early Archaean or Hadean. The amphibolite melting model of ref. 8 would predict a clustering of eclogite residues with superchondritic Nb/Ta ratios, which is not observed; instead, eclogites interpreted as residues of TTG magmatism display a wide range of Nb/Ta ratios, reflecting the variability of their basaltic (that is, oceanic) crustal source. Thus the complementarity between TTG granitoids and eclogite residues is primarily 'east-to-west', and not 'north-to-south', as the amphibolite melting model would predict. The field for MORB, mid-ocean ridge basalt, is bounded by the blue curve.

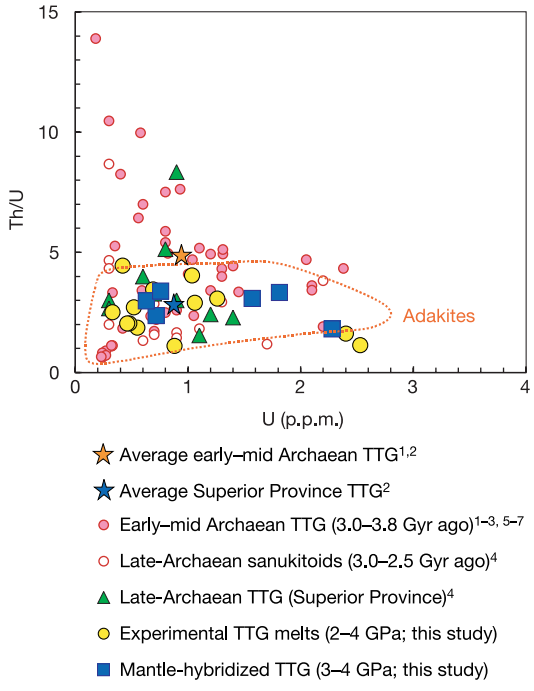

Figure 2 Variations of Th/U versus U in Archaean TTG are also consistent with their equilibration with eclogitic residues. Data are shown for both 'pristine' and 'mantle-hybridized' TTG melts formed at 2–4 and 3.5–4.0 GPa, respectively, measured by ion microprobe and laser-ablation ICP-MS, and for early–mid-Archaean TTG, late-Archaean TTG and sanukitoids (Mg-rich monzodiorites[4]) from the Slave and Superior provinces of Canada.

Table 1 **Abundances of trace elements in starting material and TTG melts**

Sample	Nb	Ta	Nb/Ta	Zr	Sm	Zr/Sm
Bulk AB-1	3.2 ± 0.1	0.51 ± 0.01	6.3	80 ± 2	2.99 ± .01	26.7
Melt of AB-1 ($n = 3$)	5.4 ± 0.6	0.7 ± 0.2	7.7	272 ± 15	4.5 ± 0.5	60
Melt of AB-1 + 15%DP ($n = 3$)	9.7 ± 0.1	1.4 ± 0.1	6.9	320 ± 30	7.7 ± 1.1	42
Melt of AB-1 + 12%FP ($n = 3$)	11.4 ± 0.3	1.5 ± 0.1	7.6	358 ± 10	7.3 ± 0.2	49

DP, depleted peridotite; FP, fertile peridotite. Data given for pristine and mantle-hybridized TTG melts of basalt (AB-1) at 3.8 GPa.

(Fig. 3). The actual process causing fractionation of Nb from Ta and leading to subchondritic Nb/Ta ratios remains a contentious issue[9,10,13]. One possible explanation involves subduction-related metasomatism of depleted oceanic lithosphere of the mantle wedge by slab-derived fluids possessing low Nb/Ta, acquired by equilibration with rutile-bearing oceanic crust[9,25]. In this scenario, the partition coefficient for Nb between rutile and aqueous fluids is higher than that for Ta, imparting a low Nb/Ta ratio to the fluid. Subsequent melting of this fluid-metasomatized, depleted oceanic mantle lithosphere would produce basalts with variable but generally subchondritic Nb/Ta ratios, representing possible mafic sources for TTG magmas (Fig. 3).

Low- to moderate-degree (5–30%) melting of basalt AB-1 at 3–4 GPa produces TTG liquids with low Nb/Ta ratios and elevated Zr/Sm ratios (the latter being due to higher partition coefficients for Sm in clinopyroxene relative to Zr), in equilibrium with rutile-bearing eclogite residues. The variable but generally low Nb/Ta and high Zr/Sm ratios of Archaean TTG can be explained by partial melting of oceanic basalt with variable but generally sub-chondritic Nb/Ta ratios, leaving residues consisting of eclogite which also possess low but variable Nb/Ta (Fig. 3). The presence of residual rutile raises the Nb/Ta ratio of the partial melt of AB-1 only slightly, due to the somewhat higher D for Ta relative to Nb in rutile in the presence of granitoid melts[25]. From mass balance considerations, we estimate that rutile-TTG melt D values are ~55–60 for Nb, and 85–90 for Ta, with a $D^{\mathrm{Nb/Ta}} \approx 0.68$, comparable to previous estimates[25] of $D^{\mathrm{rutile/melt}} \approx 27$ for Nb and $D^{\mathrm{rutile/melt}} \approx 44$ for Ta, with a $D^{\mathrm{Nb/Ta}} \approx 0.60$–$0.67$. It appears that the $D^{\mathrm{rutile/melt}}$ used in ref. 8 in modelling melting of rutile-bearing eclogite were much higher, especially for Nb; combined with a starting material with an assumed chondritic Nb/Ta ratio, their calculations suggested that partial melting of rutile-bearing eclogite would result in TTG liquids with superchondritic Nb/Ta. Note, however, that the subchondritic Nb/Ta ratios of our experimental eclogite residues are comparable to those of rutile-bearing eclogites previously interpreted as being residues from TTG magma generation[26,27]. The generally subchondritic (but highly variable) Nb/Ta ratios of Archaean TTG, consequently, require neither an amphibolitic source[8], nor a hidden eclogitic reservoir with superchondritic Nb/Ta (ref. 28), complementary to 'average' Archaean TTG (with subchondritic Nb/Ta) and linked to continent formation. We argue that the use of an 'average' Nb/Ta ratio for Archaean TTG is misleading, since the complementary nature of TTG and their eclogitic residues spans a broad range of Nb/Ta ratios, reflecting the compositional diversity of their basaltic source material.

Models for the origin and growth of the continental crust and the chemical evolution of the subcratonic lithosphere in the Archaean require a general understanding of the genetic relationship between TTG granitoids comprising the earliest continental masses, and their deep roots or 'keels' in the underlying mantle. Our results suggest that some eclogitic xenoliths and inclusions in diamonds from the subcratonic mantle may indeed represent residues from partial melting and TTG magmatism[26,27,29]. The source for Archaean TTG magmas may have been oceanic crust with variable Nb/Ta ratios, formed in a variety of environments in association with intraoceanic subduction; tectonic imbrication and accretion of these disparate terranes would have led to partial melting and TTG magmatism at the base of overthickened, juvenile arc crust[15,16]. We see TTG magmas, then, as the result of a process that begins with tectonic thickening of oceanic crust in a subduction-style regime, followed by progressive metamorphism and partial melting of metabasaltic sources, initially composed of amphibolite and garnet amphibolite, but culminating in TTG liquids that for the most part were in equilibrium with anhydrous eclogite residues, before mobilization and emplacement in evolving granite-greenstone complexes that would ultimately form the first continents. □

Methods

Melting experiments on hydrous basalts produce TTG liquids over a broad pressure interval (1–4 GPa), corresponding to the breakdown of water-bearing minerals (primarily amphibole, but also zoisite, lawsonite and phengite). Our own experiments were conducted on natural amphibolitic rock powders in the piston-cylinder apparatus ($P = 1.8$–3.2 GPa; refs 18, 20) or the multi-anvil apparatus ($P = 3.5$–3.8 GPa; ref. 19), at temperatures and pressures close to or beyond the amphibole-out phase boundary[20]. At the P–T conditions of the experiments, partial melting produces 10–30% (by weight) TTG liquid coexisting with eclogite (garnet + Na-rich clinopyroxene) residues containing minor amounts (~0.5–1.0 wt%) of rutile, and with amphibole either absent, or present as a minor phase in the lower-pressure experiments[18,20]. In related experiments in the multi-anvil apparatus at 3.8 GPa, 'pristine' TTG liquids produced by partial melting of metabasalt at 1,100 °C were allowed to infiltrate and react with an overlying layer of natural peridotite, producing 'mantle-hybridized' TTG liquids in equilibrium with garnet websterite reaction residues (garnet + orthopyroxene ± clinopyroxene)[19].

Selected trace elements were measured in the granitoid liquids produced in these experiments, using primarily the ion microprobe, with a number of samples also analysed by laser-ablation ICP-MS. From limited ion probe analyses of coexisting crystalline phases, mineral-melt partition coefficients (D values) between TTG melts and eclogitic (garnet and clinopyroxene) residues were also determined (R.P.R. and N.S., manuscript in preparation). Mineral-melt D values between garnet and TTG liquids, and between clinopyroxene and TTG liquids, measured at natural abundance levels, are similar to those previously published for "doped" experiments for a broad range of trace elements[21–23]. These measurements not only provide an independent test of Henry's law behaviour, but more importantly, they indicate that the abundances of trace elements measured in the TTG liquids formed in rock-melting experiments represent equilibrium concentrations, imposed by the crystal-chemical partitioning effects of the dominant phases (garnet and clinopyroxene).

One of the metabasalt compositions used in our experiments (AB-1) comes from extrusive sequences of the Josephine ophiolite complex of northern California and Oregon, which is interpreted as having formed by episodic spreading in a Late Jurassic back-arc basin. This particular sample has an initial Nb/Ta ratio of ~6.3 (Nb = 3.2 ± 0.1 p.p.m.; Ta = 0.51 ± 0.01 p.p.m.), and an initial Zr/Sm ratio of ~27 (Zr = 80 ± 2 p.p.m.; Sm = 2.99 ± 0.01 p.p.m.), as determined by solution ICP-MS (Table 1). Although we suspect that some contamination with respect to Ta may have taken place years ago during initial crushing of the sample in tungsten carbide (G. Harper, personal communication, 2002), artificially lowering the Nb/Ta ratio, this has no effect over the partitioning of these elements between solid and liquid phases during partial melting (essentially representing a slight doping of the basaltic source with Ta, at near-natural abundance levels).

With regard to estimates of mineral-melt D values between rutile and TTG liquids for Ta and Nb, we have shown that melts in equilibrium with amphibolite-dominated crystalline residues possess higher A/CNK ratios than those in equilibrium with eclogitic residues (the tonalite in the experiments of ref. 8 has a peraluminous A/CNK of ~1.15, compared to metaluminous A/CNK ratios of ~1.0 in our experiments. We believe that our estimated rutile-melt D values for Nb and Ta are much more reasonable values, because D values for Nb and Ta between rutile and granitoid melts have been shown to be strongly dependent on melt composition, and decrease dramatically as liquid composition changes from peraluminous to metaluminous[30].

Received 23 March; accepted 28 August 2003; doi:10.1038/nature02031.

1. Martin, H. Adakitic magmas: modern analogues of Archean granitoids. *Lithos* **46,** 411–429 (1999).
2. Smithies, R. H. The Archean tonalite-trondhjemite-granodiorite (TTG) series is not an analogue of Cenozoic adakite. *Earth Planet. Sci. Lett.* **182,** 115–125 (2001).

3. Hunter, D. R., Smith, D. G. & Sleigh, D. W. W. Geochemical studies of Archean granitoid rocks in the Southeastern Kaapvaal Province: implications for crustal development. *J. Afr. Earth Sci.* **15,** 127–151 (1992).
4. Feng, R. & Kerrich, R. Geochemical evolution of granitoids from the Archean Abitibi southern volcanic zone and the Pontiac subprovince, Superior Province, Canada: implications for the tectonic history and source regions. *Chem. Geol.* **98,** 23–70 (1992).
5. Luais, B. & Hawkesworth, C. J. The generation of continental crust: an integrated study of crust-forming processes in the Archean of Zimbabwe. *J. Petrol.* **35,** 43–93 (1994).
6. Nutman, A. P., Bennett, V. C., Friend, C. R. L. & Norman, M. D. Meta-igneous (non-gneissic) tonalites and quartz-diorites from an extensive ca. 3800 Ma terrain south of the Isua supracrustal belt, southern West Greenland: constraints on early crust formation. *Contrib. Mineral. Petrol.* **137,** 364–388 (1999).
7. Kreissig, K., Nagler, T. F., Kramers, J. D., van Reenen, D. D. & Smit, C. A. An isotopic and geochemical study of the northern Kaapvaal Craton and the Southern Marginal Zone of the Limpopo Belt: are they juxtaposed terranes? *Lithos* **50,** 1–25 (2000).
8. Foley, S., Tiepolo, M. & Vannucci, R. Growth of early continental crust controlled by melting of amphibolite in subduction zones. *Nature* **417,** 637–640 (2002).
9. Niu, Y. & Batiza, R. Trace element evidence from seamounts for recycled oceanic crust in the Eastern Pacific mantle. *Earth Planet. Sci. Lett.* **148,** 471–483 (1997).
10. Weyer, S., Munker, C. & Mezger, K. Nb/Ta Zr/Hf and REEs in the depleted mantle: implications for the differentiation history of the crust-mantle system. *Earth Planet. Sci. Lett.* **205,** 309–324 (2003).
11. Bedard, J. H. Petrogenesis of boninites from the Betts Cove Ophiolite Newfoundland, Canada: identification of subducted source components. *J. Petrol.* **40,** 1853–1889 (1999).
12. Cluzel, D., Aitchison, J. C. & Picard, C. Tectonic accretion and underplating of mafic terranes in the Late Eocene intraoceanic forearc of New Caledonia (Southwest Pacific): geodynamic implications. *Tectonophysics* **340,** 23–59 (2001).
13. Munker, C. Nb/Ta fractionation in a Cambrian arc/back arc system. New Zealand: source constraints and application of refined ICPMS techniques. *Chem. Geol.* **144,** 23–45 (1998).
14. Nicholson, K. N., Picard, C. & Black, P. M. A comparative study of Late Cretaceous ophiolitic basalts from New Zealand and New Caledonia: implications for the tectonic evolution of the SW Pacific. *Tectonophysics* **327,** 157–171 (2000).
15. de Wit, M. J. On Archean granites, greenstones, cratons, and tectonics: does the evidence demand a verdict? *Precambr. Res.* **91,** 181–226 (1998).
16. Kusky, T. M. & Polat, A. Growth of granite-greenstone terranes at convergent margins, and stabilization of Archean cratons. *Tectonophysics* **305,** 43–73 (1999).
17. Sen, C. & Dunn, T. Dehydration melting of a basaltic composition amphibolite at 1.5 and 2.0 GPa: implications for the origin of adakites. *Contrib. Mineral. Petrol.* **117,** 394–409 (1994).
18. Rapp, R. P. & Watson, E. B. Dehydration melting of metabasalt at 8–32 kbar: implications for continental growth and crust-mantle recycling. *J. Petrol.* **36,** 891–931 (1995).
19. Rapp, R. P., Shimizu, N., Norman, M. D. & Applegate, G. S. Reaction between slab-derived melts and peridotite in the mantle wedge: experimental constraints at 3.8 GPa. *Chem. Geol.* **160,** 335–356 (1999).
20. Rapp, R. P. Amphibole-out phase boundary in partially melted metabasalt, its control over liquid fraction and composition, and source permeability. *J. Geophys. Res.* **100,** 15601–15610 (1995).
21. Barth, M. G., Foley, S. F. & Horn, I. Partial melting in Archean subduction zones: constraints from experimentally determined trace element partition coefficients between eclogitic minerals and tonalitic melts under upper mantle conditions. *Precambr. Res.* **113,** 323–340 (2002).
22. Klein, M., Stosch, H.-G., Seck, H. A. & Shimizu, N. Experimental partitioning of high field strength and rare earth elements between clinopyroxene and garnet in andesitic to tonalitic systems. *Geochim. Cosmochim. Acta* **64,** 99–115 (2000).
23. Klemme, S., Blundy, J. D. & Wood, B. J. Experimental constraints on major and trace element partitioning during partial melting of eclogite. *Geochim. Cosmochim. Acta* **66,** 3109–3123 (2002).
24. Boily, M. & Dion, C. Geochemistry of boninite-type volcanic rocks in the Frotet-Evans greenstone belt. Opatica subprovince, Quebec: implications for the evolution of Archean greenstone belts. *Precambr. Res.* **115,** 349–371 (2002).
25. Green, T. H. Significance of Nb/Ta as an indicator of geochemical processes in the crust-mantle system. *Chem. Geol.* **120,** 347–359 (1995).
26. Jacob, D. E. & Foley, S. F. Evidence for Archean ocean crust with low high field strength element signature from diamondiferous eclogite xenoliths. *Lithos* **48,** 317–336 (1999).
27. Barth, M. G. *et al.* Geochemistry of xenolithic eclogites from West Africa. Part I: A link between low MgO eclogites and Archean crust formation. *Geochim. Cosmochim. Acta* **65,** 1499–1527 (2001).
28. Rudnick, R. L., Barth, M., Horn, I. & McDonough, W. F. Rutile-bearing refractory eclogites: missing link between continents and depleted mantle. *Science* **287,** 278–281 (2000).
29. Rollinson, H. Eclogite xenoliths in west African kimberlites as residues from Archean granitoid crust formation. *Nature* **389,** 173–176 (1997).
30. Horng, W-S. & Hess, P. C. Partition coefficients of Nb and Ta between rutile and anhydrous haplogranite melts. *Contrib. Mineral. Petrol.* **138,** 176–185 (2000).
31. Polat, A., Hofmann, A. W. & Rosing, M. T. Boninite-like volcanic rocks in the 3.7–3.8 Ga Isua greenstone belt, West Greenland: geochemical evidence for intra-oceanic subduction zone processes in the early Earth. *Chem. Geol.* **184,** 231–254 (2002).

Acknowledgements This research was supported by National Science Foundation grants to R.P.R. and the Mineral Physics Institute at Stony Brook. We thank M. Defant for critical comments. Discussions with H. Martin, A. Polat, H. Rollinson, M. Rosing, H. Smithies and M. de Wit helped to improve the manuscript.

Competing interests statement The authors declare that they have no competing financial interests.

Correspondence and requests for materials should be addressed to R.P.R. (rrapp@notes.cc.sunysb.edu).

Large Cretaceous sphenodontian from Patagonia provides insight into lepidosaur evolution in Gondwana

Sebastián Apesteguía & Fernando E. Novas

Museo Argentino de Ciencias Naturales "Bernardino Rivadavia", Av. Ángel Gallardo 470, Buenos Aires (1405), Argentina

Sphenodontian reptiles successfully radiated during Triassic and Jurassic times, but were driven almost to extinction during the Cretaceous period[1]. The sparse Early Cretaceous record of sphenodontians has been interpreted as reflecting the decline of the group in favour of lizards, their suspected ecological successors[2]. However, recent discoveries in Late Cretaceous beds in Patagonia partially modify this interpretation. Numerous skeletons of a new sphenodontian, *Priosphenodon avelasi* gen. et sp. nov., were collected from a single locality in the Cenomanian–Turonian Candeleros Formation, where it is more abundant than any other tetrapod group recorded in the quarry (for example, Crocodyliformes, Serpentes, Dinosauria and Mammalia)[3,4]. Adult specimens of *Priosphenodon* reached one metre in length, larger than any previously known terrestrial sphenodontian. Here we propose, using available evidence, that sphenodontians were not a minor component of the Cretaceous terrestrial ecosystems of South America, and that their ecological replacement by squamates was delayed until the early Tertiary. The new discovery helps to bridge the considerable gap in the fossil record (around 120 million years) that separates the Early Cretaceous sphenodontians[5–7] from their living relatives (*Sphenodon*).

Today, lepidosaurs are a diverse group of reptiles. With more than 6,000 species of lizard, snake, amphisbaenian and tuatara, they form an important part of the terrestrial vertebrate fauna. Although the evolutionary history of lepidosaurs during the late Mesozoic is relatively well known in North America and Asia, their record in the Southern Hemisphere (Gondwana) is very limited. As a result, basic questions about their evolutionary history remain incompletely answered, including the origin of snakes, the biogeography of iguanian lizards, the origin of basal squamates and the relictual presence of *Sphenodon*, the last sphenodontian, in New Zealand, an isolated part of Gondwana.

New findings presented below, including well-preserved and abundant skeletons of a new sphenodontian collected from Cenomanian–Turonian[8] rocks in North Patagonia, permit a better understanding of some aspects of late Mesozoic lepidosaurian evolution in the southern continents.

Lepidosauria Haeckel, 1866 (ref. 9)
Sphenodontia Williston, 1925 (ref. 10)
Opisthodontia nov.
Eilenodontinae Rasmussen & Callison, 1981 (ref. 11)
Priosphenodon avelasi gen. et sp. nov.

Holotype. MPCA 300 (Museo Carlos Ameghino, Cipolletti, Río Negro Province, Argentina) consists of a partially articulated, adult skeleton (Fig. 1a–c).

Referred material. The present study was based on the holotype as well as the following specimens: MPCA 301, a juvenile incomplete skeleton (Fig. 1d, e); MPCA 302, postcranial isolated remains (Fig. 1g, h); and MPCA 303, a partially articulated adult skeleton. More than a hundred uncatalogued specimens, including isolated elements and complete skeletons, remain unprepared.